Microelectronic Engineering 86 (2009) 83–87

Contents lists available at ScienceDirect

Microelectronic Engineering

journal homepage: www.elsevier.com/locate/mee

Reduction of polarization and swing effects in a high numerical aperture exposure system by utilizing resist antireflective coatings

H.L. Chen [a,*], W.H. Lee [a], Wonder Fan [b], S.Y. Chuang [a], Y.H. Lai [c], C.C. Lee [c]

[a] Department of Materials Science and Engineering, National Taiwan University, 1, Sec. 4, Roosevelt Road, Taipei 106, Taiwan
[b] National Nano Device Laboratory, Hsinchu, Taiwan
[c] Department of Optics and Photonics, National Central University, Taiwan

ARTICLE INFO

Article history:
Received 29 April 2008
Received in revised form 16 September 2008
Accepted 28 September 2008
Available online 25 October 2008

Keywords:
Swing effects
Polarization effects
High numerical aperture
Exposure system
Resist antireflective coatings

ABSTRACT

Exposure systems having high numerical apertures (NAs) are essential for increasing the resolution of optical lithography. The efficiency of conventional single-layer bottom antireflective coating (BARC) structures, however, degrades as the angle of incidence increases. In this paper we demonstrate a multilayer BARC structure for high-NA systems employed in ArF lithography. Because the reflection difference between transverse electric (TE or s) and transverse magnetic (TM or p) polarization at the air–resist interface results in low image contrast for high-NA exposure systems, we also describe a single-layer top antireflective coating (TARC) layer that can be used to reduce the polarization effect. By combining the optimized TARC and multilayer BARC structures, the swing effect can be alleviated and the image contrast can be improved for angles of incidence ranging from 0° to 70° (i.e., NA = ca. 0.93).

1. Introduction

The recent International Technology Roadmap for Semiconductors reported that high numerical aperture (NA) ArF exposure systems combined with liquid immersion and resolution enhancement technologies have great potential to lead IC technologies to the generation of sub-45 nm features [1–3]. The problems of critical dimension control caused by highly reflective substrates are far more serious in this spectral regime than at the longer wavelength. The efficiency of conventional single-layer antireflective coating structures degrades as the angle of incidence increases because of increased reflectance. It is, therefore, necessary to develop high-performance antireflective coating layers that can be used in high-NA exposure systems. In this paper, we demonstrate a multilayer bottom antireflective coating (BARC) layer for high-NA exposure systems employed in ArF lithography. This multilayer antireflective structure comprises conventional silicon oxynitride films [4]. By adding an optimized structure, the reflectance at the resist-silicon substrate interface can be maintained to less than 1% for angles of incidence ranging from 0° to 70° (i.e., NA = ca. 0.93).

In general, p-polarized light reduces the image contrast because the electric field vectors are not aligned parallel and cannot interfere completely, as indicated in Fig. 1 [2,3]. In a high-NA exposure tool, this polarization effect is more serious when the angle of incidence of the light approaches the Brewster angle. In this study, we developed a single-layer top antireflective coating (TARC) layer, which, when used in conjunction with the multilayer BARC, solves the problems of both the polarization and swing effects in high-NA ArF lithography.

2. Simulation and experimental setup

The swing ratio is defined as the intensity variation within a resist. There are two primary approaches toward reducing the interfacial reflection of a resist: using a TARC layer and using a BARC layer. These layers are designed to minimize reflection at the air–resist (R_1) and resist–substrate (R_2) interfaces, respectively. Assuming that the resist is a weak absorption layer, the refractive index (n_{TARC}) and thickness (d_{TARC}) of a TARC layer that are required to minimize the value of R_1 at an angle of incidence θ can be obtained using the following equation [5]:

$$n_{\mathrm{TARC}} = \sqrt{n_{\mathrm{Resist}}} \quad \text{and} \quad d_{\mathrm{TARC}} = \frac{\lambda}{4 \cdot n_{\mathrm{TARC}} \cdot \cos\theta} \tag{1}$$

In a multilayer BARC, the extinction coefficient of each BARC layer gradually increases, with the highest value at the bottom. The combination of multilayer thin film stacks causes a gradual change in the optical constants, resulting in minimal reflectance at each BARC layer interface. Thus, a graded-absorption multilayer

---

[*] Corresponding author. Tel.: +886 2 33663240; fax: +886 2 23634562.
E-mail address: hsuenlichen@ntu.edu.tw (H.L. Chen).

0167-9317/$ - see front matter © 2008 Elsevier B.V. All rights reserved.
doi:10.1016/j.mee.2008.09.050

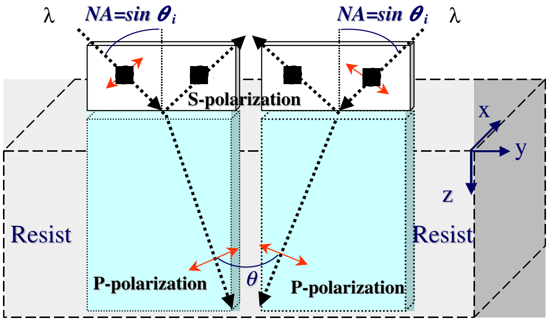

Fig. 1. Electric field vectors of p-polarized light are not parallel and cannot completely interfere.

BARC can be used in various reflective substrates [6]. The optimal single-layer and multilayer BARC structures can be determined using optical thin film theory [7].

Among many theoretical systems for studying periodic structures, two-beam interference within a resist film is the simplest when modeling lithographic systems. We focused on the determining the efficiency of reduction of polarizing effects in high-NAs and examined the behavior of structures at various angles of incidence using a two-beam interference system. We employed vector theory, which defines the image distribution in terms of Joule heat. The exposure is defined as $Q \times t$, where t is the exposure time and the absorbed energy Q represents the form of the recorded image distribution within the resist. Using this approach allows the image distributions for s- and p-polarization illumination to be determined [8]. Table 1 displays the optical constants and various ARC structures designed for high-NA lithography.

The silicon oxynitride and oxide films were deposited for the BARC structures by employing a conventional high-density-plasma chemical vapor deposition (HDP-CVD) system (BR-2000LL). The optical constants of the BARC films were obtained by utilizing the R-T method and an ellipsometer. The reflectance spectra were measured using an optical spectrometer (Hitachi, U 4100). The weakly absorbing resist was DHA-1000 (Dongjin Semichem). The simulation tools Film Wizard (Scientific Computing International) and Matlab (MathWorks, Inc.) were used to evaluate the polarization effects and the dependence of the resist profile on the angle of incidence.

3. Results and discussion

Fig. 2a reveals that the reflection of s- and p-polarized light at air–resist interface was dependent on the angle of incidence. The

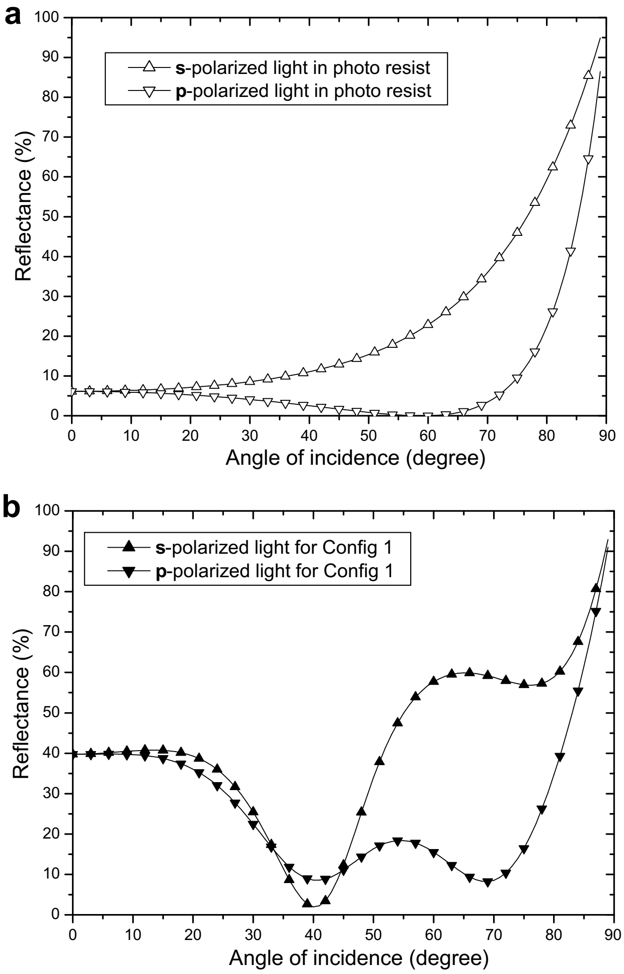

Fig. 2. Reflections of s- and p-polarized light at the (a) air–resist interface (b) air–resist–silicon dependence on the numerical aperture.

Table 1
Optical constants and various ARC structures designed for high-NA lithography.

Configuration	Film assembly					
	Ambient	N_{TARC}	N_{PR}	N_{BARC}	d_{TARC}	Note
1	Air	–	1.659–0.019i	–	–	Without TARC and BARC
2	Air	1.288	1.659–0.019i	–	54 nm	With TARC for NA = 0.93
3	Air	–	1.659–0.019i	1.850–0.301i 1.831–0.560i 1.850–1.002i	–	Multilayer BARC
4	Air	1.288	1.659–0.019i	1.850–0.301i 1.831–0.560i 1.850–1.002i	54 nm	Multilayer BARC and TARC for NA = 0.93
5	Air	–	1.659–0.019i	1.831–0.560i	–	Single-layer BARC
6	Air	1.288	1.659–0.019i	1.850–0.301i 1.831–0.560i 1.850–1.002i	40 nm	Multilayer BARC and TARC for NA = 0.50
7	Air	1.288	1.659–0.019i	1.850–0.301i 1.831–0.560i 1.850–1.002i	37 nm	Multilayer BARC and TARC for NA = 0.20
8	Water	–	1.659–0.019i	1.850–0.301i 1.831–0.560i 1.850–1.002i	–	Liquid immersion

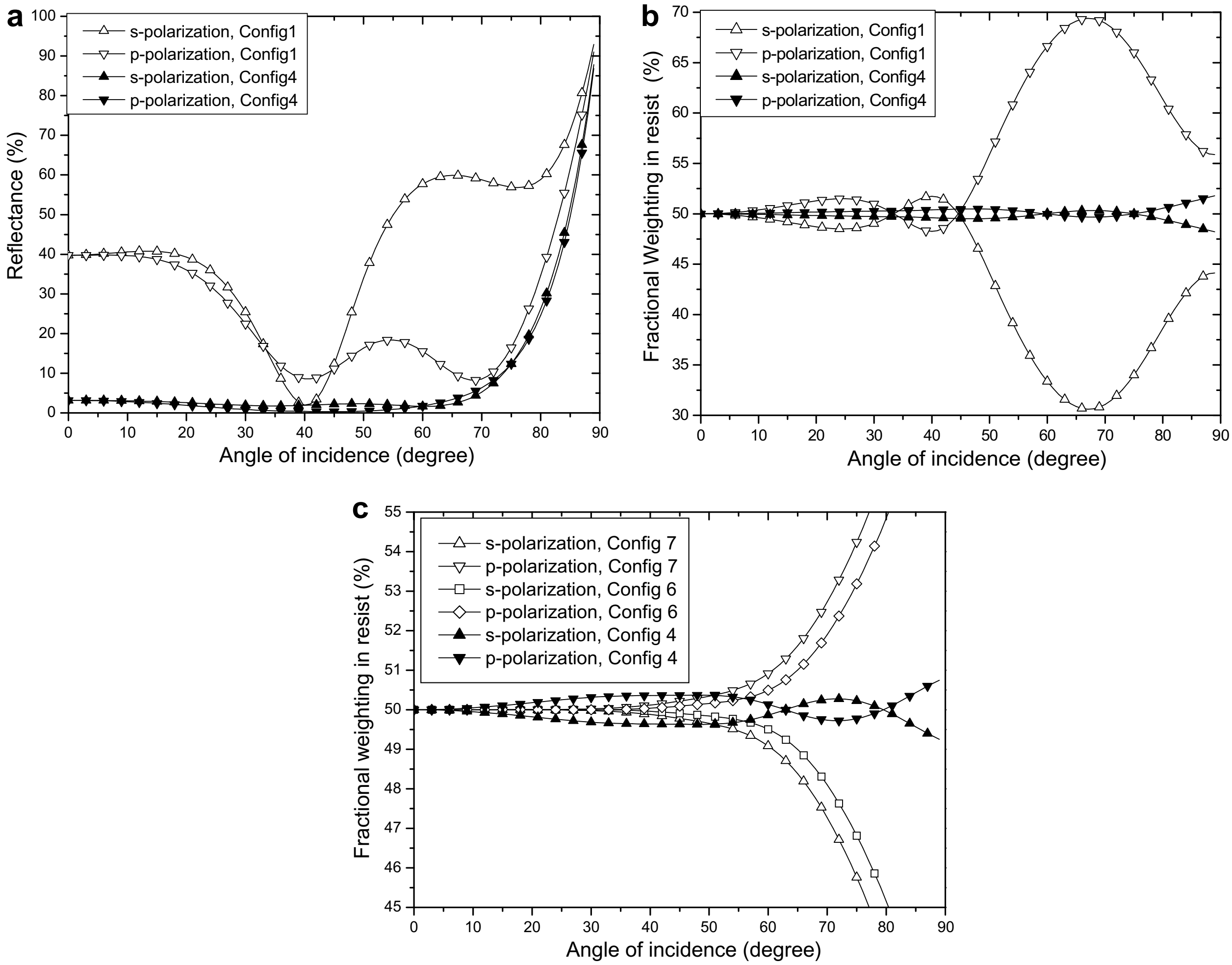

Fig. 3. (a) Reflections of s- and p-polarized light in the presence and absence of a TARC layer. (b) Fractional weighting in the resist dependence on the angle of incidence in the presence and absence of a TARC layer. (c) Fractional weighting in resists featuring TARC structures designed for NAs of 0.20, 0.50, and 0.93.

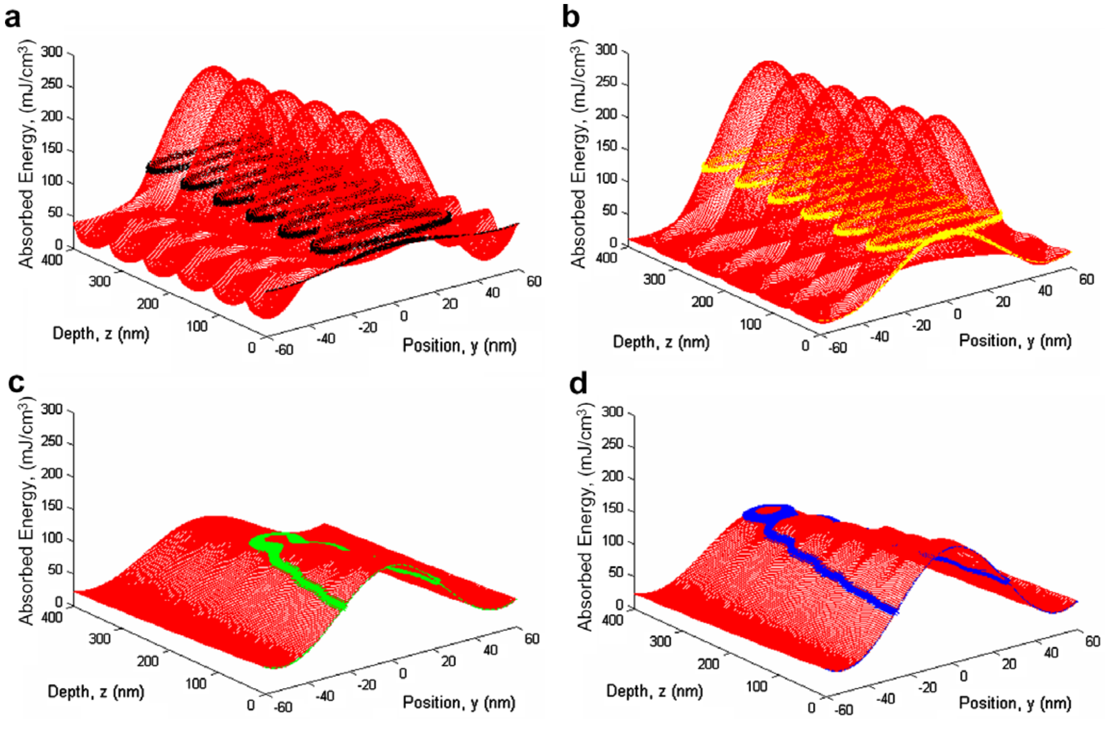

Fig. 4. Energy distributions in resists having configurations (a) 1, (b) 2, (c) 3, and (d) 4.

reflection of s-polarized light was greater than that of the p-polarized light when the angle of incidence was close to the Brewster angle. Fig. 2b displays the reflection of light from the air–resist–silicon substrate having a resist layer thickness of 400 nm. When considering the thin film interference effect, the Brewster angle phenomenon becomes imperceptible, although the reflection of s-polarized light remained larger than that of p-polarized light at large angles of incidence. This behavior indicates that the ratio of incident p-polarized light is weighed more substantially than that of s-polarized light in the resist as the NA increases. Therefore, we sought to develop a strategy for reducing polarization effects in high-NA exposure systems.

In this study we investigated the use of a single-layer TARC to reduce polarization effects. According to thin film theory, we designed some optimal TARC structures for exposure tools featuring values of NA of 0.20, 0.50, and 0.93; Table 1 presents the structures. Fig. 3a reveals that the reflections of s- and p-polarized light were dependent on the angle of incidence in both the presence and absence of a single-layer TARC, but they were reduced significantly for angles of incidence ranging from 0° to 70° when the single-layer TARC was present. Fig. 3b presents the fractional polarization weightings in the resist in the absence and presence of the TARC layer. After adding a TARC designed for a value of NA of 0.93, the fraction of s- to p-polarized light in the resist was ca. 49% over the range of angles of incidence from 0° to 70°. Furthermore, Fig. 3c displays the fractional polarization weightings in the resist featuring a single-layer TARC designed for the angles of incidence of 70° (NA = 0.93), 30° (NA = 0.50), and 12° (NA = 0.20). The TARC designed for 70° exhibited the best performance for reducing the difference between the s- and p-polarization reflections over the range of angles of incidence ranging from 0° to 80°. Therefore, we propose that the polarization effect can be reduced by adding a single-layer TARC that has been designed for the largest NA of the exposure tool.

Different configurations of TARC and BARC structures result in differences in the amount of energy absorbed within a resist. Using the theory of two-beam vector interference, Fig. 4 displays the energy distribution within resists having four different configurations. For the structure lacking both the TARC and the BARC (configuration 1), a significant swing effect resulted from reflections at both the air–resist and resist–substrate interfaces. A significant swing effect also appeared in configuration 2, because a single-layer TARC alone cannot minimize the reflection from highly reflective substrates in the high-NA regime. In contrast, the swing effect was reduced significantly when only a multilayer BARC structure was present. The swing effect vanished and more energy was transferred into the resist when a single-layer TARC and a multilayer BARC structure were combined. Therefore, although multilayer BARC structures are more important than TARC layers for reducing the swing effect in high-NA lithography, the TARC structure does help the resist to absorb more energy from both s- and p-polarized light.

To analyze the effect of a TARC layer on the image contrast, we calculated the energy distributions within the resist at various focus positions [9]. Fig. 5a reveals that the image contrasts for configuration 3 (i.e., a structure possessing a multilayer BARC but no TARC layer) did not vary at different focus positions, but it did decrease upon increasing the angle of incidence. Similarly, Fig. 5b reveals that the image contrasts of configuration 4 (a structure possessing both a multilayer BARC and a TARC layer) designed for the NA of 0.93 did not vary perceptibly. Furthermore, the image contrast for configuration 4 was better than that of configuration 3, especially for the NA of 0.93. Thus, a TARC layer can alleviate the polarization effect in the high-NA regime.

Silicon oxynitride-based single-layer and multilayer BARC structures are added to reduce the reflectance at the interface between a silicon substrate and a resist. Thin film theory suggests that the reflectance at normal incidence can be reduced to 0.5% when using a single-layer or multilayer structure. As indicated in Fig. 6a, the reflections of both the single-layer and multilayer structures increased slowly upon increasing the angle of incidence, but the reflectance of the multilayer BARC structure remained at less than 1% over the range of angles of incidence from 0° to 90° (i.e., NA from 0 to 1). Thus, the multilayer BARC structure provided superior performance to that of the single-layer structure for high-NA exposure systems.

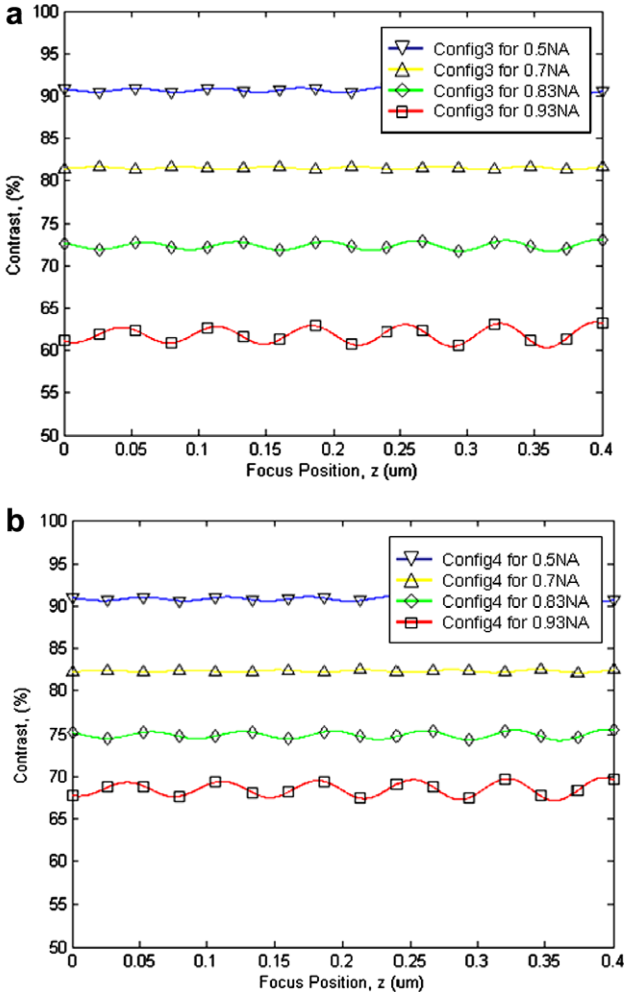

Fig. 5. Effects of the focus positions and NA on the image contrast of resists in the (a) absence and (b) presence of a TARC layer.

To analyze the effect of different BARC structures on the image contrast, we calculated the energy distributions within resists at various focus positions. Configuration 1 is the structure lacking a BARC; configurations 3 and 5 are structures possessing multilayer and single-layer BARCs, respectively. Fig. 6b displays the image contrasts of configurations 1, 3, and 5 for the NA of 0.93. In the absence of a BARC structure, the image contrasts of configuration 1 varied significantly at the different focus positions. By adding BARC structures, the variations in contrast were reduced dramatically [Fig. 6b], with the contrast variation of configuration 3 being smaller than that of configuration 5 for the NA of 0.93. In addition, the multilayer BARC structure provided superior contrast performance to that of the single-layer structure in high-NA exposure systems. Fig. 6c presents the contrast variations of a multilayer BARC for immersion lithography (configuration 8) with NAs of 0.7, 1.0, and 1.3. In the presence of a multilayer BARC structure, the image con-

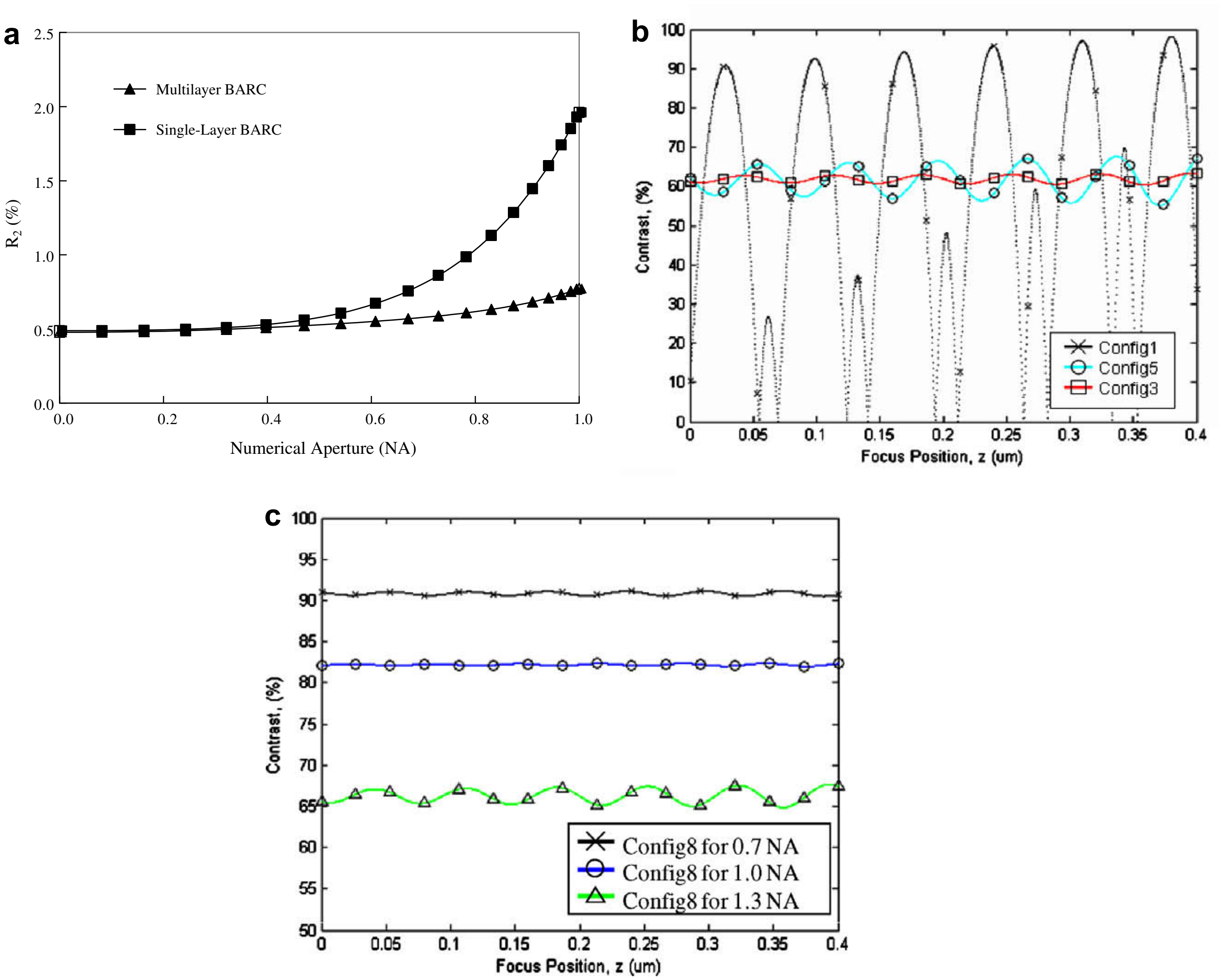

Fig. 6. (a) Effect of the NA on the reflectance at the resist–substrate interfaces of single-layer and multilayer BARCs. (b) Effects of BARC structures and focus positions on the contrast dependence. (c) Contrast variations of a multilayer BARC used in immersion lithography with various NAs.

trast did not vary perceptibly at the different focus positions upon increasing the NA from 0.7 to 1.3, suggesting that the multilayer BARC would also be suitable for application in liquid immersion lithography.

4. Conclusion

The use of exposure systems with high-NA is essential to increasing the resolution of optical lithography. The efficiency of the conventional single-layer BARC structure degrades as the angle of incidence increases. We have developed a multilayer BARC layer for high-NA exposure systems used in ArF lithography. By adding the optimized structure, the reflectance can be maintained to less than 1% for angles of incidence ranging from 0° to 70° (i.e., NA = ca. 0.93). The swing effect in the resist is also reduced significantly. Additionally, the reflection separation of s- and p-polarized light at the air–resist interface results in low image contrast for high-NA lithography. We also found that a single-layer TARC can be used to reduce the polarization effect. By combining the optimized TARC and multilayer BARC structures, the swing effect can be alleviated and the image contrast can be improved for angles of incidence ranging from 0° to 70°. The multilayer BARC is also suitable for application in liquid immersion lithography.

Acknowledgment

We thank the National Science Council, Taiwan, R.O.C., for supporting this study under projects NSC-95-2221-E-002-324-MY2 and NSC-96-2623-7-002-005-ET.

References

[1] International Technology Roadmap for Semiconductors, 2006 (Updated).
[2] T.A. Brunner, N. Seong, et al., SPIE 4691 (2002) 1–10.
[3] B.W. Smith, J. Cashmore, SPIE 4691 (2002) 11–24.
[4] T.A. Brunner et al., SPIE 4346 (2001) 1050.
[5] T. Perera, Solid State Technol. 7 (1995) 131.
[6] L.A. Wang, H.L. Chen, J. Vac. Sci. Technol. B 17 (1999) 2772.
[7] H.A. Macleod, Macmillan, New York, 1986.
[8] D.G. Flagello, T.D. Milster, Appl. Opt. 36 (1997) 8944.
[9] C.S. Williams, O.A. Becklund, Introduction to the Optical Transfer Function, John Wiley & Sons, 1989.